Crossref
Similarity Check
Powered by iThenticate

Orginal Article

FEM model versus laboratory test of thin-walled steel beams strengthened by CFRP tapes

Katarzyna Rzeszut[1], Ilona Szewczak[2], Patryk Różyło[3]

[1] *Institute of Building Engineering; Poznan University of Technology;*
Marii Skłodowskiej-Curie St.5, 60-965 Poznań, Poland;
katarzyna.rzeszut@put.poznan.pl **iD** *0000-0002-7134-608X*
[2] *Faculty of Civil Engineering and Architecture; Lublin University of Technology;*
Nadbystrzycka St. 38 D, 20–618 Lublin, Poland;
i.szewczak@pollub.pl **iD** *0000-0002-4953-0104*
[3] *Faculty of Mechanical Engineering; Lublin University of Technology;*
Nadbystrzycka St. 38 D, 20–618 Lublin, Poland;
p.rozylo@pollub.pl **iD** *0000-0003-1997-3235*

Abstract: The main aim of the study is to develop the best-suited FEM numerical model of beams made of thin-walled cold-rolled steel profiles retrofitted by CFRP tapes. The FEM model fitting has been carried out based on own laboratory tests conducted on Σ type beams. The CFRP tapes are bonded to the beam at compressed or tensioned flange. The most important part of this study is focused on the investigation of boundary conditions influence in FEM model developed in Abaqus program. Moreover, the numerical models are also tested in terms of different mesh density and type of finite elements. Numerical analyses are carried out using a Newton-Raphson iterative method to solve the non-linear equilibrium equation. In the paper, special attention is paid to the evaluation of the possibility to increase the load capacity by appropriate localisation of CFRP tape.

Keywords: steel thin-walled cold-formed beam, CFRP tape, strengthening

1. Introduction

New technological solutions require a special approach, namely before their introduction to common use, ant that means experimental studies should precede them. Nevertheless, due to the high costs of laboratory tests, they are usually carried out for a very narrow spectrum of cases, while broader analyses are made using the so-called numeric experiment. For this purpose, it is very important to carry out the verification and validation of the FEM numerical model as

well as possible. This problem has recently become extremely important in order to verify the innovative methods of retrofitting the steel thin-walled cold-rolled elements, which have been widely used in civil engineering not only as purlins or rails but also as main structural bearing elements. One can notice that due to very thin walls, these structures are characterised by a limited possibility of reinforcement methods because traditional ones, such as welding or bolted connection, are not very efficient. Therefore, it is necessary to look for a smart and accurate method to overcome the problem of strengthening the existing steel elements with very thin walls.

One of many options is the use of tapes made of carbon fibre reinforced polymers (CFRP); they enable fast and effective reinforcement of the structure practically without limiting the continuity of its operation. CFRP tapes are characterised by excellent mechanical properties such as over ten times higher strength in tension of the tape in fibres direction compared with conventional structural steel grades and high fatigue or corrosion resistance. These properties depend on the type and the orientation of carbon fibres, the type of the epoxy resin, and its percentage share in the final material. The disadvantage of CFRP tapes is low strength in compression, which is approximately 10% of the tensile strength. Strength parameters of FRP materials used to strengthen structures are described in detail in [13]. However, the main advantage of CFRP tape in case of thin-walled structures is the possibility to applicate an adhesive bond between CFRP tape and construction, which allow for an easy and speedy connection without the damage of very thin steel walls. The detailed information on rules of adhesive bonding in steel, aluminium, and composite structures is presented in [9], [8].

Research papers on reinforced steel elements subjected to bending or compression are being presented in scientific reports more and more frequency. Research on steel circular hollow section (CHS) confirms that using CFRP for strengthening deficient columns showed the appropriate impact on rising bearing capacity and reducing stress in the damaged location and preventing local deformation [7]. Also, positive conclusions are drawn from the analysis of the steel squared hollow section (SHS) restrained with CFRP tapes [4]. In addition, as shown in [5], CFRP tapes allow for the reinforcement of corroded steel elements. It was shown that the combined flexural and bearing capacity of the CHS could be significantly increased by adhesively bonding CFRP. The maximum gain in strength was 434%, which was obtained for the most severe 80% corrosion, extended along the full length. In engineering practice, CFRP tapes are used to reinforce steel bridge girders, which is justified by Ardalani et al. in [3], or I-beams used, for example, as floor beams. CFRP materials can also be used to reinforce steel floor beams with holes in the web, as discussed in [1]. In this paper, an experimental study involving four full-scale beams under 6-point bending was carried out. The study was conducted to investigate the ability of CFRP to improve the load-bearing capacity of beams with web opening. As a result, up to 20% increase in the bearing capacity of the elements was achieved. CFRP materials also found application for reinforcement of aluminium structures. In [14], which is based on the example of the pre-stressed aluminium bridge, the authors showed that the application of the extruded CFRP tendon-anchor system provides an improvement of 25%. The abovementioned references indicate the wide use of modern composite materials for reinforcement of various types of steel structures. Still, the use of CFRP composites to strengthen steel structures is incomparably small, in relation to the use of these materials in the reinforcement of concrete or masonry structures. It should be emphasised that there are very few studies on strengthening thin-walled steel structures by CFRP. This fact became

the motivation for the authors to undertake research regarding the strengthening of sigma thin-walled steel elements with CFRP tapes. Authors of this paper paid particular attention to the evaluation of the possibility of increasing the load capacity of the thin-walled beams by appropriate position of CFRP tape. The work involved verification and validation of different FEM numerical models of thin-walled sigma profile strengthen with CFRP tapes using the Abaqus / CAE program and solid or finite shell elements.

2. Laboratory tests

The scope and course of laboratory tests, as well as the obtained test results, were discussed in detail in [11] and [12]. Laboratory tests were carried out on sigma thin-walled, cold-rolled beams. The dimensions of the cross-section of the sigma profile was $\sum$140x70x2.5. All tested beams were simply supported elements with the span of 2.20 m and loaded by uniformly distributed load using laboratory stand prepared in accordance with the patent [10]. The uniformly distributed load was applied to the sample using steel cables in seven points along the span of the beam. The displacement of each beam was measured using the four displacement gauges – three in the horizontal direction and one in the vertical direction, placed in the middle of the span. In the case of five beams, a measurement of strain was made using six strain electrofusion gauges TENMEX TFs-10, the resistance of 120 Ω ± 0.2%. Experimental studies were carried out in the Laboratory of Civil Engineering, in Lublin University of Technology, in the test machine Zwick & Roel controlling the growth of the load specified by the extending press piston with a speed of 1 mm/min, recording the force at 0.01 s. The scheme of the laboratory stand, the geometry of the cross-section of the tested beams and are shown in Fig. 1.
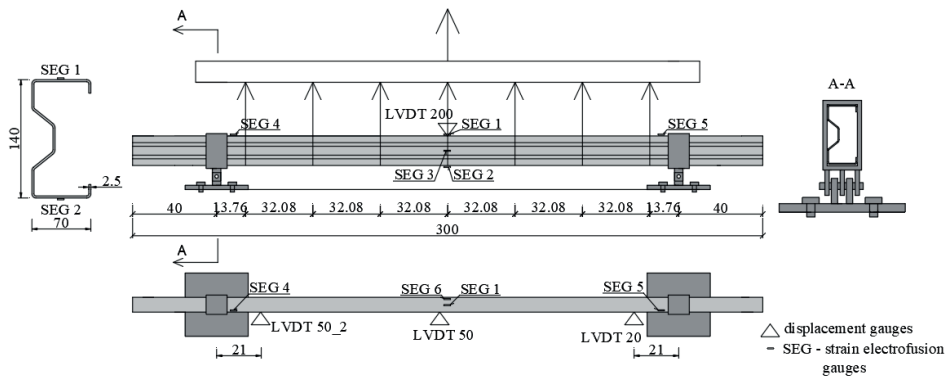

Fig. 1.   Scheme of the laboratory stand and the geometry of the tested beams. *Source:* own study

On the basis of the σ-ε relationship obtained in laboratory coupon test, the bilinear elastic-plastic material model with strain hardening with Young's modulus (201.8 GPa), Poisson's ratio (0.282), and yield strength (418.5 MPa) was adopted in FEM numerical model (Fig. 2). Lower value of Young's modulus than for the S350 GD steel grade, results from the fact that the samples are made of galvanised steel.
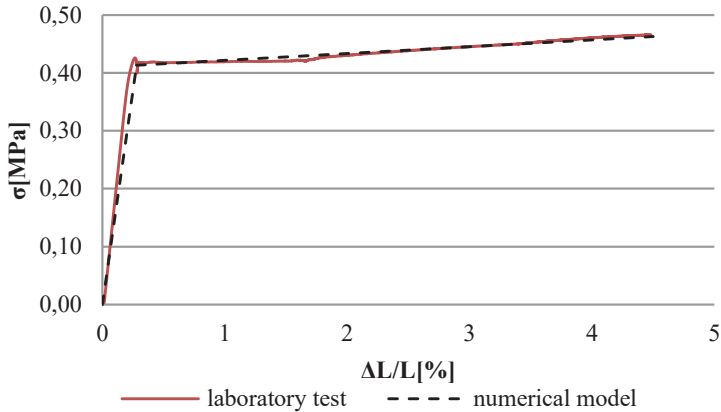
Fig. 2.   Material characteristics of steel: laboratory coupon test; numerical model. Source: own study

The CFRP tapes, with a thickness of 1.2 mm and width of 50 mm, were described as orthotropic material with typical composite materials characteristic such as Young's modulus (165 GPa) and Poisson's ratio (0.308).

3. Numerical model

Various numerical models in FEM program ABAQUS®[1] were developed. In order to select the most suitable one, they were subjected to calibration based on own laboratory test results [11]. Numerical analyses were performed for beams identical to those tested in the laboratory. Namely, for simply supported, subjected to uniformly distributed load elements with the span of 2.20 m and made of Σ140x2.5 cross-section. In the numerical model, the load was defined in the same way as in the experiment, taking into account that the load is transmitted by means of seven steel cables along the length of the beam. Numerical models corresponding to beams tested in the laboratory were considered. Beam "B3" was not reinforced (bare beam). Beam "B4" was reinforced by CFRP tape bonded to the external surface of the tensioned flange, while beam "B1" to the internal surface of the compressed flange. The layout of CFRP tapes in the examined beams adopted in laboratory tests and a numerical model is shown in Fig. 3.
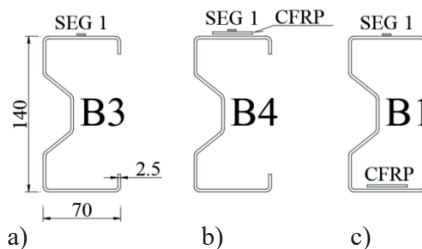

Fig. 3.   Layout of CFRP tapes on the examined thin-walled beams a) bare beams, b) CFRP tape bonded to the tensioned flange, c) CFRP tape bonded to the compressed flange. *Source:* own study

Connection between the CFRP tapes and the corresponding plane (the lower and upper flange) of the beam was modelled using a numerical TIE-type connection. Another method of modelling adhesive connection can be found in [6]. The developed numerical models were different in terms of boundary conditions, the type of finite element (FE) and mesh size. The summary of the analysed numerical models is presented in Tab. 1.

Table 1.   Summary of the analysed numerical models. *Source:* own study

No.	Acronym of num. model	Type of boundary conditions	Type of FE	Number of FE/ nodes
1.	*Abaqus solid B3p*	Non-deform. shell el. R3D4	SOLID C3D8R	45000/61404
2.	*Abaqus solid B3k*	Displacement constraints	SOLID C3D8R	45000/61404
3.	*Abaqus shell B3l.p*	Non-deform. shell el. R3D4	SHELL S4R	46200/46878
4.	*Abaqus shell B3l.k*	Displacement constraints	SHELL S4R	46200/46878
5.	*Abaqus shell B3k.p*	Non-deform. shell el. R3D4	SHELL S8R	46200/139955
6.	*Abaqus shell 3k.k*	Displacement constraints	SHELL S8R	46200/139955

Each of the MES models has been prepared, taking into account the contact properties in the tangent and normal direction, between the beam and supports.

In the numerical models, the supports were modelled in two ways, each of which described so-called fork support. In the first method, the supports were modelled by using displacement constraints imposed at the points No. 1-5 located on the contour in the plane created by the partition of the element. At points No. 1, 2, 3, and 4 transfers displacements U_x were constrained and at point No. 5 – longitudinal displacement U_y was constrained. At all this points rotation was free (Fig. 4a). In the second model, the supports were modelled using non-deformable shell elements of the R3D4 type (Fig. 4b).

Thin-walled sigma beams ware modelled using three different types of finite element, namely, a solid element with a linear shape function of the C3D8R type with 3 translational degrees of freedom in each of the 8 nodes per one finite element. Next, the shell element of S4R type with a linear shape function (four-node type with reduced integration), and finally, a shell element of S8R type with a square shape function was used.

The analysis of the influence of mesh size was made only for the numerical model No. 4 (*Abaqus shell B3l.k*) changing the size of the finite element from 5 mm to 7.5 mm. The model with a finite element size of 7.5 mm had 24 400 elements and 24862 nodes and was marked with the acronym *Abaqus shell B3l.k.g*. The next stage of the analysis consisted of removing the mesh density on the rounded corners of the profile, which resulted in the creation of a cross-section with sharp edges. This model had 21 200 elements and 21 665 nodes and was marked with the acronyms *Abaqus shell B3l.k.k*.

In order to reflect laboratory tests of beams B1 and B4, numerical models No. 1 and No. 4, were extended by the numerical modelling of CFRP tapes. In all numerical models, CFRP tapes were modelled as shell finite elements of the S8R type, which contains 6 degrees of freedom, in each of the 8 nodes per finite element. The number of finite elements was 1 040 and the number of computational nodes was 1 254. Connection between the CFRP tape and the corresponding beam surface was modelled using a "TIE" type numerical connector which preserves the constant distance between points lying on two adjacent surfaces and constraint rotations between these points.
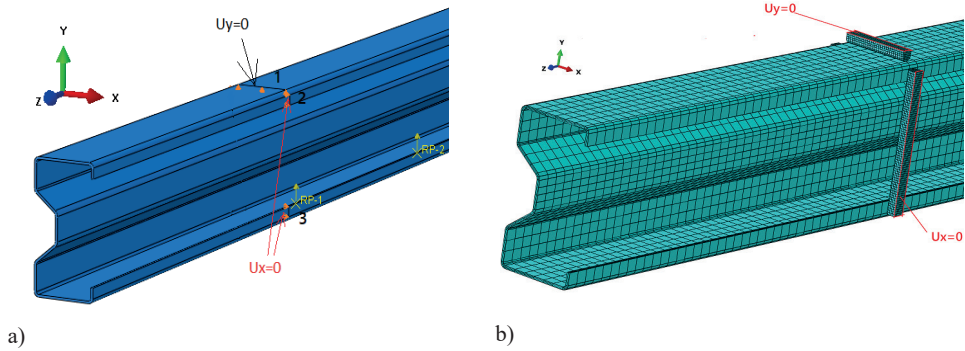
Fig. 4. Numerical models of the support a) displacement constraints: U_y, U_x. b) non-deformable shell elements R3D4 and displacement constraints: U_y, U_x. *Source:* own study

Another parameter that has a decisive influence on numerical results is the size of the mesh in the numerical model. In order to investigate this effect, the mesh size analysis was performed for a numerical model with S4R shell finite elements, linear shape function and supports modelled as displacement constraints. As it was mentioned above, the size of the mesh was changed from 5 mm (Abaqus shell B3l.k) to 7.5 mm (Abaqus shell B3l.k.g). The next modification was to remove the increase mesh density on the rounded surfaces of the element. Thus, a simplified model was created with a finite element size of 7.5 mm and constant mesh density (Abaqus shell B3l.k.k). Various mesh configuration in numerical models are presented in Fig. 5.
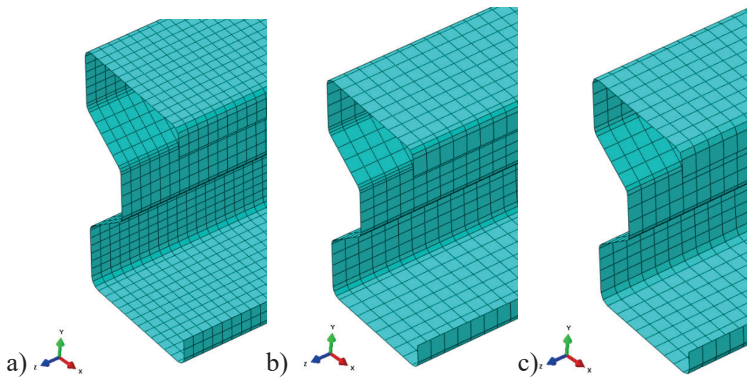

Fig. 5. Various mesh configuration in numerical models: a) *Abaqus shell B3l.k*, b) *Abaqus shell B3l.k.g*, c) *Abaqus shell B3l.k.k. Source:* own study

The non-linear studies are carried out by solving the equilibrium equation. The Newton-Raphson iterative method is used for both stable and unstable post-buckling responses.

4. Results of numerical analysis versus laboratory test

As mentioned before, in order to find the best representation of the real structural behaviour, numerical models differing in terms of modelling boundary conditions, mesh density and finite element types have been developed. FEM model quality assessment was conducted by

comparison of strain measured during laboratory tests by electrofusion strain gauge SEG 1, SEG 2, placed in the middle of the beam span, in the centre of the tensile or compressed flange respectively, with results obtained from the FEM analysis. Unfortunately, due to the significant rotation of the beam, the displacement measurement was not reliable, because the induction gauges did not remain in constant contact with one measuring point (Fig. 6).
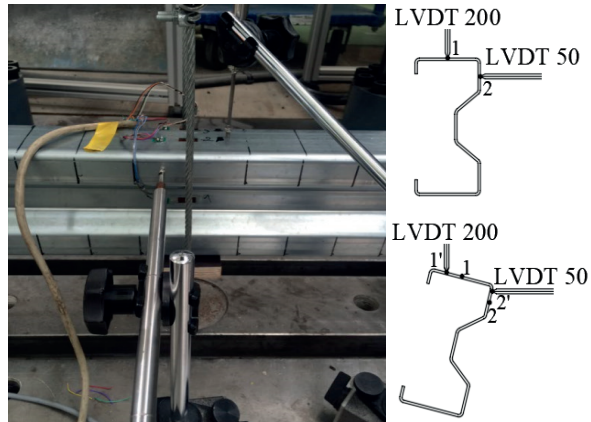

Fig. 6.   Displacement measurements details. *Source:* own study

Therefore, this parameter was not taking into account during the evaluation of the numerical model.

Comparison of the *P-ε* relationship for different numerical models (see Tab. 1) and laboratory test (plot *B3*) for the bare beam (without reinforcement) shows Fig. 7.
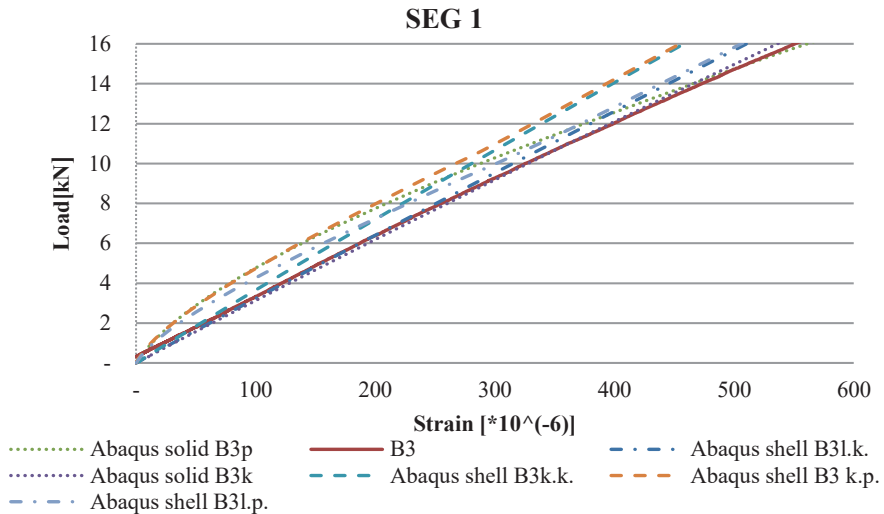

Fig. 7.   The *P-ε* (load – strain) relationship for the bare beam (SEG 1 readout) for laboratory specimen and various numerical models. *Source:* own study

The analysis of the obtained results shows that the highest compliance with the results of laboratory tests was obtained for two numerical models. Namely, for the numerical modelled using solid FE with a linear shape function (*Abaqus solid B3k*) and for a numerical model with shell FE and linear shape function (*Abaqus shell B3l.k*). In these two models, supports were modelled by using displacement constraints. One can notice that the numerical model (*Abaqus solid B3k*) shows compatibility over the whole equilibrium path while the numerical model (*Abaqus solid B3k*) loses its convergence at a higher load level. Noteworthy is also the numerical model (*Abaqus solid B3p*) with solid FE and the supports in the form of non-deformable shell elements R3D4. This model is characterised by very good convergence for the maximum load value. However, the worst compatibility is observed in the case of a beam modelled by shell-type FE with a square shape function and supports in the form of non-deformable shell elements R3D4 (*Abaqus shell B3k.p*).

Based on the above observations, three models were selected for further analysis (*Abaqus solid B3k*, A*baqus solid B3p and Abaqus shell B3l.k*). Thus, in the case of beams strengthened with CFRP tape, the validation and verification were limited only to three numerical models. In Fig. 5 the relationship *P*-ε (load – strain) for the beam strengthened with CFRP tapes based on SEG 1 laboratory readout and results obtained for selected numerical models is presented.

In Fig. 8a the plot *B4* refers to the beam strengthened with CFRP tapes bonded to the tensioned flange tested in the laboratory and the other plots illustrate the response of the beam strengthened in the same way for three representative numerical models (*Abaqus solid B4k, Abaqus solid B4p, Abaqus shell B4l.k*). Fig. 8b presents the strain values read from SEG 1 for beams strengthened with CFRP tape at compressed flange (B1) and analogous numerical model (*Abaqus solid B1k, Abaqus solid B1p, Abaqus shell B1l.k*).

One can notice that in case of the beams strengthened with CFRP tapes at the tensioned or compressed flange the highest compliance with the results of laboratory tests occurs for numerical models with shell or solid FE and displacement constraints (*Abaqus shell B1l.k, Abaqus solid B1k, Abaqus shell B4l.k and Abaqus solid B4k*). This conclusion coincides with the observations made for unreinforced beams. Surprisingly, the most complex numerical model (*Abaqus solid B1p and Abaqus solid B4p*) in the initial phase of the work of the beam provides results that deviate from the laboratory tests.
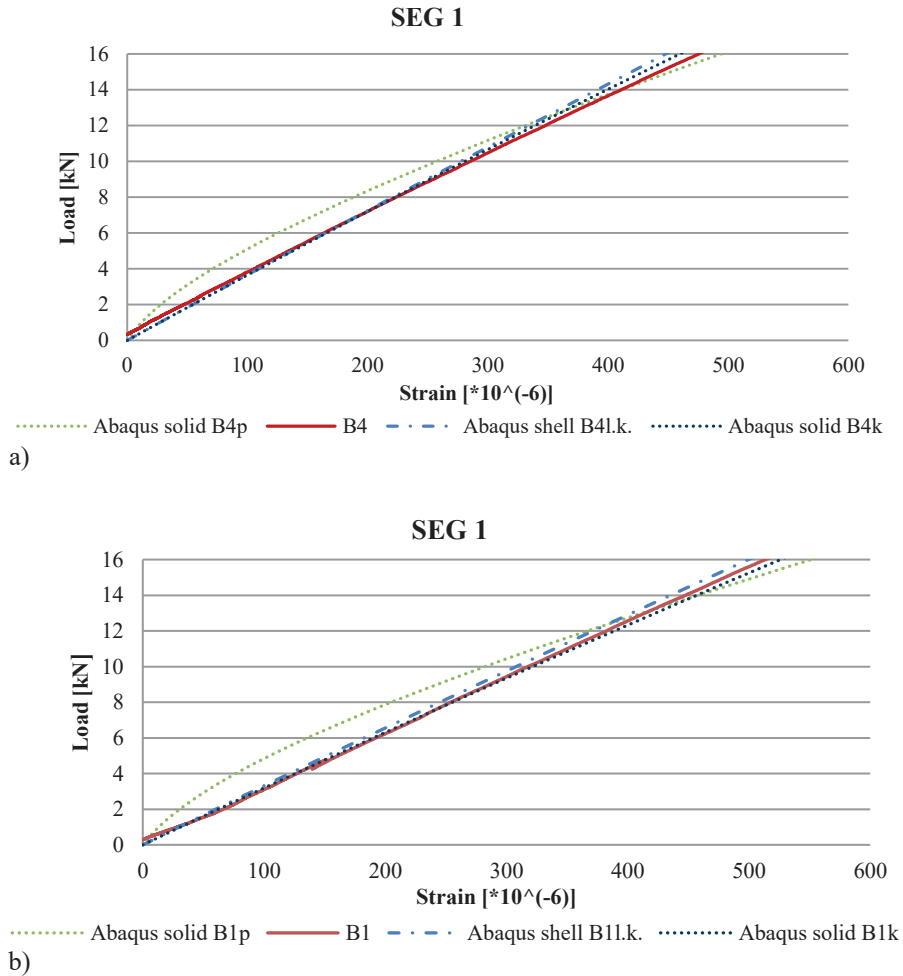
a)

b)

Fig. 8. The load – strain relationship (SEG 1 readout) for laboratory specimen and various numerical models for the strengthen beam: a) at the tensioned flange, b) at the compressed flange. *Source:* own study

The force – strain relationship obtained for the bare beams for different mesh size in numerical model and SEG 1 readout in laboratory tests is presented in Fig. 9. For the beam restrained by CFRP tape bonded to the tensioned flange (B4) the mesh size analysis (Fig. 10) was performed for the numerical model (*Abaqus shell B4 l.k.k, Abaqus shell B4l.k*). Analogous, the force – strain relationship for beams reinforced with CFRP tape at compressed flange (B1) and the numerical model (*Abaqus shell B1l.k.k, Abaqus shell B1 l.k*) is shown in Fig. 11.
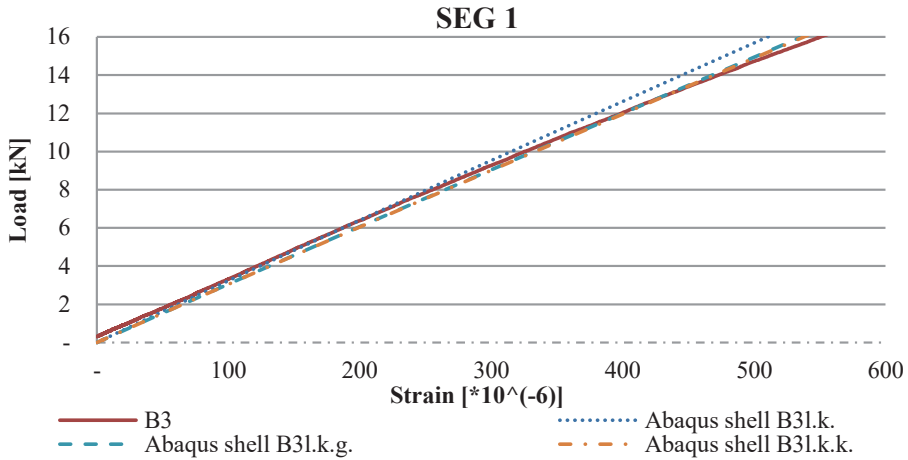
Fig. 9.   The force – strain relation obtained from the numerical model and SEG 1 readout for the bare beams for different mesh size. *Source:* own study
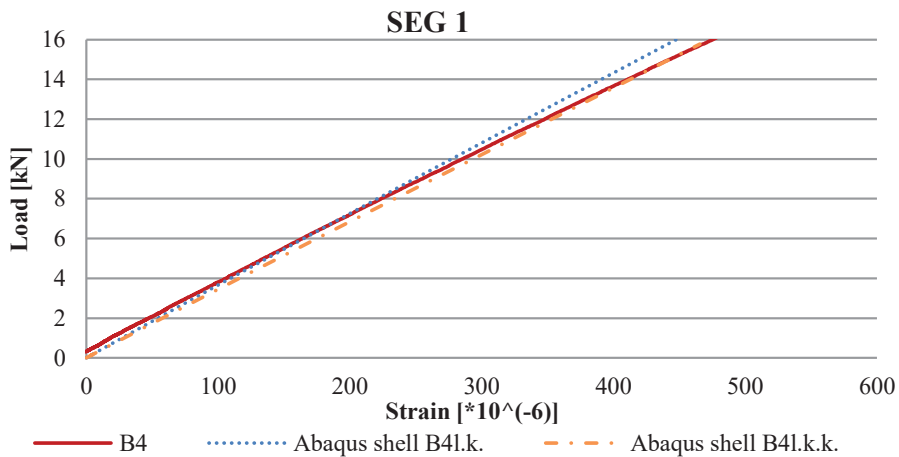

Fig. 10.   The force – strain relation obtained from the numerical model and SEG 1 readout for the beams reinforced at the tensioned flange. *Source:* own study
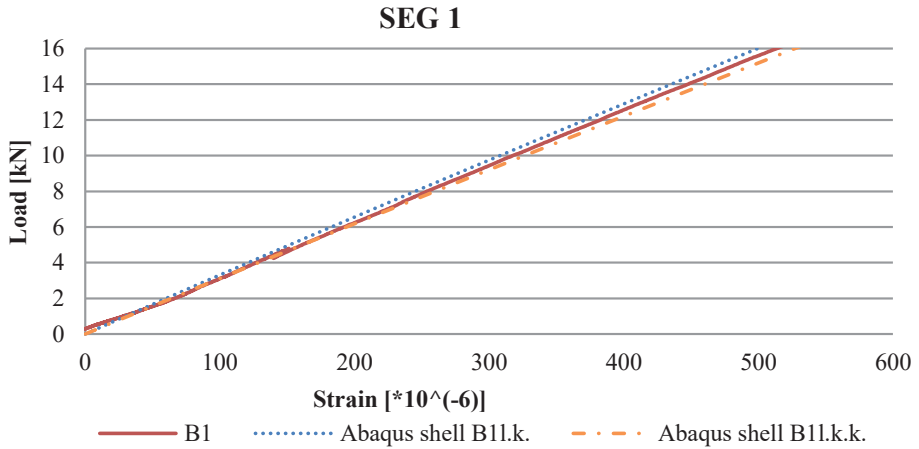
SEG 1

Fig. 11.   The force – strain relation obtained from the numerical model and SEG 1 readout for the beams reinforced at compressed flange. Source: own study

The force – strain relationship obtained for the bare beams and the beams reinforced at the tensioned flange for different mesh size in the numerical model and SEG 2 readout in laboratory tests is presented in Fig. 12 and 13.
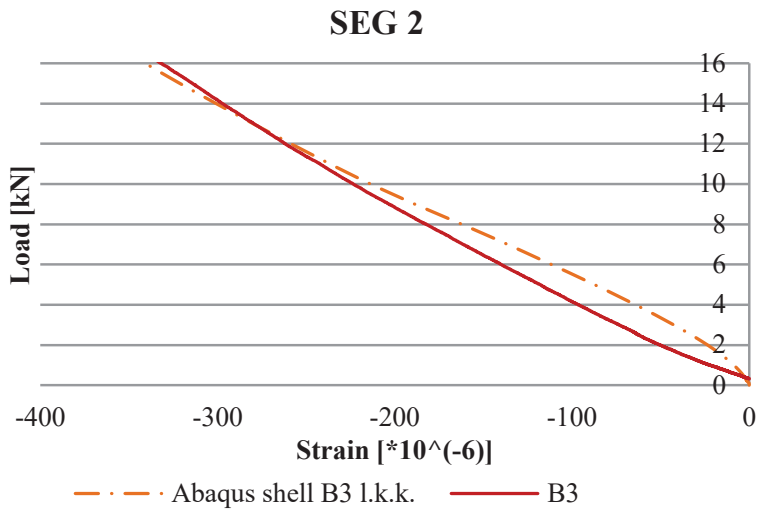
SEG 2

Fig. 12.   The force – strain relation obtained from the numerical model and SEG 2 readout for the bare beams for different mesh size. *Source:* own study
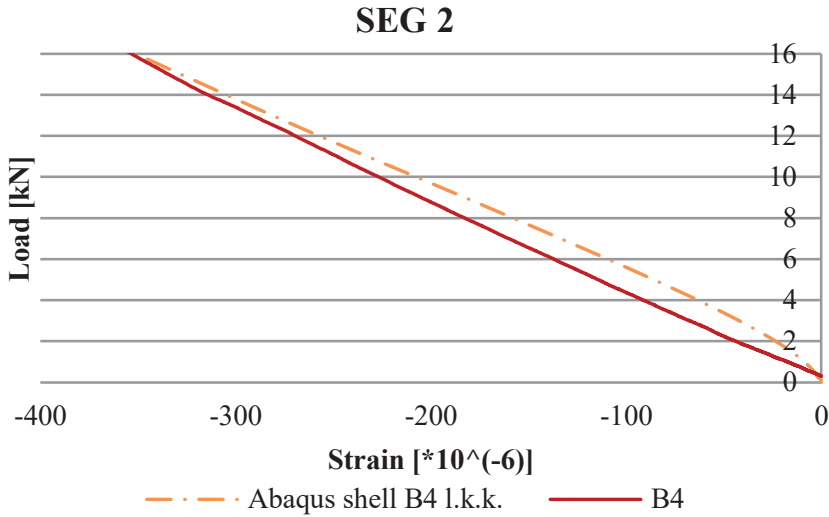
Fig. 13. The force – strain relation obtained from the numerical model and SEG 1 readout for the beams reinforced at the tensioned flange. *Source:* own study.

5. Concluding remarks

The research presented in the paper is of a pilot nature and is part of a more extensive program. The primary purpose of the work was to check the efficiency of strengthening sigma beams using CRP tape in the context of laboratory and numerical tests. The primary conclusion of the presented article highlights the difficulties associated with the analysis of the field of displacement and deformation of beams subjected to significant rotation.

The original purpose of the laboratory tests was to analyse beams that undergo significant rotation. Unfortunately, the used laboratory stand made it impossible and eliminate the possibility to carry out the experiment until the damage. Therefore, in order to track the behaviour of the beam reinforced with CFRP tapes over the entire load range. A numerical model was created to reproduce the laboratory conditions as accurately as possible by introducing the appropriate contact and non-linear analysis.

Conducted analyses allowed to conclude that the results most similar to laboratory tests were obtained for the model with supports modelled in a simplified way by using displacement constraints. Numerical model with supports modelled as non-deformable shell elements produced significant discrepancies, which is surprising, because it faithfully reflects the real laboratory conditions. Based on the obtained results, it can be stated that laboratory tests most accurately describe the numerical model (*Abaqus shell B3l.k.k, Abaqus shell B4l.k.k, Abaqus shell B1l.k.k*). This was unexpected because it is the least detailed numerical model. It should be noted that the above results of numerical research concerned beams without geometrical imperfections, which in the real thin-walled section can significantly affect the results.

In terms of the discrete models used, the C3D8R model was based on correlations of the results obtained with experimental studies (the use of the C3D20R mesh) in this case gave less convergent results, although it is this mesh that usually allows to obtain better qualitative and quantitative results. In the case of C3D8R mesh, 3 elements were applied to the thickness of the structure, allowing to create a neutral layer. Probably, it would have been better to use

the C3D20R mesh; however, less convergence of results was obtained for such test model than the C3D8R finally used with 3 elements on the thickness of the structure. Thus, it was found that in the case of static analysis, the least appropriate is the shell model with a square shape function.

References

[1]   Altaee M.J., Cunningham L., Gillie M., "Experimental investigation of CFRP-strengthened steel beams with web openings", *Journal of Constructional Steel Research*, Vol. 138/November 2017, pp.750-760. https://doi.org/10.1016/j.jcsr.2017.08.023

[2]   App 1 to PN-90/B-03200 "Stability parameters of structure", *Konstrukcje stalowe. Obliczenia statyczne i projektowanie.*

[3]   Ardalani G.T., Showkati H., Teymourlouei H.E., Firouzsalari S.E., "The performance of plate girders reinforced with CFRP plates of various lengths", *Thin-Walled Structures*, Vol. 120/ November 2017, pp.105-115. https://doi.org/10.1016/j.tws.2017.08.015

[4]   Bambach M.R., "Strengthening of thin-walled (hollow) steel sections using fibre-reinforced polymer (FRP) composites", in *Rehabilitation of Metallic Civil Infrastructure Using Fiber Reinforced Polymer (FRP) Composites Types Properties and Testing Methods*, eds. M. Karbhari, 2014, pp.140–168. https://doi.org/10.1533/9780857096654.2.140

[5]   Elchalakani M. et al., "CFRP strengthening and rehabilitation of corroded steel pipelines under direct indentation", *Thin-Walled Structures*, Vol. 119/ October 2017, p.510-521. https://doi.org/10.1016/j.tws.2017.06.013

[6]   Kawecki B., Podgórski J., „Analiza pracy wspornikowej belki kompozytowej z uwzględnieniem różnej grubości i lokalizacji spoiny klejowej wykonanej z materiału sprężysto-idealnie plastycznego", *Budownictwo i Architektura*, 15(4), 2016, pp. 195-208. https://doi.org/10.24358/Bud-Arch_16_154_19

[7]   Masoumeh K. et al., "Structural behaviors of deficient steel CHS short columns strengthened using CFRP", *Journal of Constructional Steel Research*, Vol. 138/ November 2017, pp.555-564. https://doi.org/10.1016/j.conbuildmat.2016.09.099

[8]   Pasternak H., Ciupack Y., "Eurocode – Based design rules for adhesive bonded joints", *Conference paper, Eurosteel 2011,* August 31 – September 2, 2011, Budapest, pp. 717-722.

[9]   Piekarczyk M., Grec R., "Application of adhesive bonding in steel and aluminium structures", *Archives of Civil Engineering,* LVIII, 3, 2012, pp. 309-329.

[10] Pieńko M., Robak A., "Stand for testing deformations of evenly loaded horizontal elements", Lublin University of Technology, 2015, Patent Application (21) 410025.

[11] Rzeszut K., Szewczak I., "Experimental Studies of Sigma Thin-Walled Beams Strengthen by CFRP Tapes", *International Journal of Civil, Environmental, Structural, Construction and Architectural Engineering*, Vol.11/2017, No.7, pp.888-895. ISNI:0000000091950263

[12] Rzeszut K., Szewczak I., Różyło P., "Issues of thin-walled sigma beams strengthened by CFRP tape in context of experimental and numerical study", *Engineering Transaction*, vol. 66/2018, no. 1, pp. 79–91.

[13] Technical report, „FRP Reinforcement in RC structures", Bulletin 40, September 2007. Available: https://www.iranfrp.ir/wp-content/uploads/2018/12/40-FRP-reinforcement-in-RC-structures_0-1.pdf [Access: 16 Jan 2020]

[14] Zhu P. et al., "Structural analyses of extruded CFRP tendon-anchor system and applications in thin-walled aluminium/CFRP bridge", *Thin-Walled Structures*, Vol. 127/ June 2018, p.556-573. https://doi.org/10.1016/j.tws.2018.02.0294